PRELIMINARY TESTS OF THE ELECTROSTATIC PLASMA ACCELERATOR

G. Aston* and T. Acker**
Electric Propulsion Laboratory, Inc.
Tehachapi, CA

Abstract

This report describes the results of a program to verify an electrostatic plasma acceleration concept and to identify those parameters most important in optimizing an Electrostatic Plasma Accelerator (EPA) thruster based upon this thrust mechanism. Preliminary performance measurements of thrust, specific impulse and efficiency were obtained using a unique plasma exhaust momentum probe. Reliable EPA thruster operation was achieved using one power supply.

Introduction

The lifetime of a typical commercial, communications satellite is limited by the mass of station keeping propellant which is carried on-board. For a typical communications satellite at geosynchronous altitude with a ten year useful life, it is generally true that each one second increase in specific impulse results in a station keeping propellant mass reduction of approximately one kilogram.

Arcjet and ion engine electric propulsion systems offer significantly increased specific impulse compared to chemical thrusters. The performance advantages offered by these relatively sophisticated propulsion systems, in general, outweigh the more complex spacecraft integration requirements their use imposes on the spacecraft. However, because these more advanced spacecraft propulsion systems are more complex, and costly, their use will probably be limited to the more expensive, large communication satellites.

Smaller, relatively inexpensive spacecraft are being developed for earth orbital mission applications. Although the mission lifetimes of these spacecraft are usually short (months, or one or two years), minimizing mass launched to orbit is still very important because of the low payload capability of the small launch vehicles. A need exists for an inexpensive electric propulsion thruster, with minimal complexity, but which still offers significantly improved specific impulse over chemical thruster systems.

The EPA thruster concept consists of a hollow cathode surrounded by a discharge chamber which is completely open at the end opposite the cathode. No accelerating electrodes are used and the specific impulse is a direct function of the applied discharge voltage and the propellant mass. Briefly, during thruster operation, a plasma is created by electron bombardment of the propellant gas in a plasma arc discharge which is sustained by the applied voltage between the cathode and the discharge chamber anodes. An initial start-up transient will occur in which more electrons will leave the thruster than ions. This will cause the discharge plasma to acquire a potential more positive than the ambient space plasma potential to prevent the further unbalanced loss of electrons. As the discharge plasma potential becomes more positive, ions will begin to be accelerated from the thruster. The potential difference between the discharge chamber plasma and the ambient space plasma will automatically adjust itself so that the loss rate of ions and electrons are equal; thus a neutral plasma will be exhausted from the thruster. The net ion velocity (and ultimately the specific impulse) is determined by the magnitude of this potential difference.

From the above discussion, it is apparent that the electrostatic acceleration process requires, in principle, only one power supply. Furthermore, this power supply could be the spacecraft bus since even voltages of 28 Vdc are sufficient to achieve significant plasma acceleration. The promise of thruster operation off the spacecraft bus, with minimal power interface requirements, makes the EPA thruster concept attractive for low cost small spacecraft.

The thrust producing mechanism for the EPA thruster was first discovered by chance in 1979 in the course of the extended SERT II (Space Electric Rocket Test II) test program.[1] In these tests, one of the SERT II mercury ion engines was operated in a discharge only mode without high voltage applied to the accelerator system. While operating in this mode, it was discovered that the thruster was producing a measured thrust level of 0.8 mN. Based on the measured thrust of 0.8 mN, Ref. 1 calculated a specific impulse of 300 sec. at an input power of 80 W, resulting in a thrust-to-

---

* Director, Member AIAA
** Research Engineer, Member AIAA

power ratio of 10 mN/kW for operation in this mode. The calculated 300 sec. specific impulse level was much higher than could be accounted for by simple gas dynamic expansion of heated mercury vapor.

This paper describes the results of a program to verify, through ground based tests, the electrostatic plasma acceleration concept and to identify those parameters most important in optimizing a thruster based upon this thrust mechanism.

Proof of Concept Thruster

A prototype EPA thruster was fabricated to perform verification testing of the electrostatic plasma acceleration concept. Primary thruster components included a magnetically protected plasma discharge chamber and a high current hollow cathode. Specific design details of these components are described below.

The EPA thruster discharge chamber required a magnetic field distribution which could prevent direct access to the anode electrodes by cathode electrons. In the interests of minimizing costs to this present program, a magnet retainer shell was loaned from the Jet Propulsion Laboratory (JPL). This structure was fabricated several years ago during a NASA/LeRC funded program concerned primarily with ion accelerator system development.[2] Figure 1 shows this magnet retainer shell. As can be seen from this figure, each side of the structure is lined by five rows of samarium cobalt magnets, forming a strongly diverging line cusp magnetic field distribution. This magnetic field distribution was not selected a priori as being optimum for the EPA thruster proof-of-concept tests. However, because the magnets in the retainer shell shown in Fig. 1 are water cooled, it was felt that a much wider range of operating conditions could be explored without any concern for hardware damage.

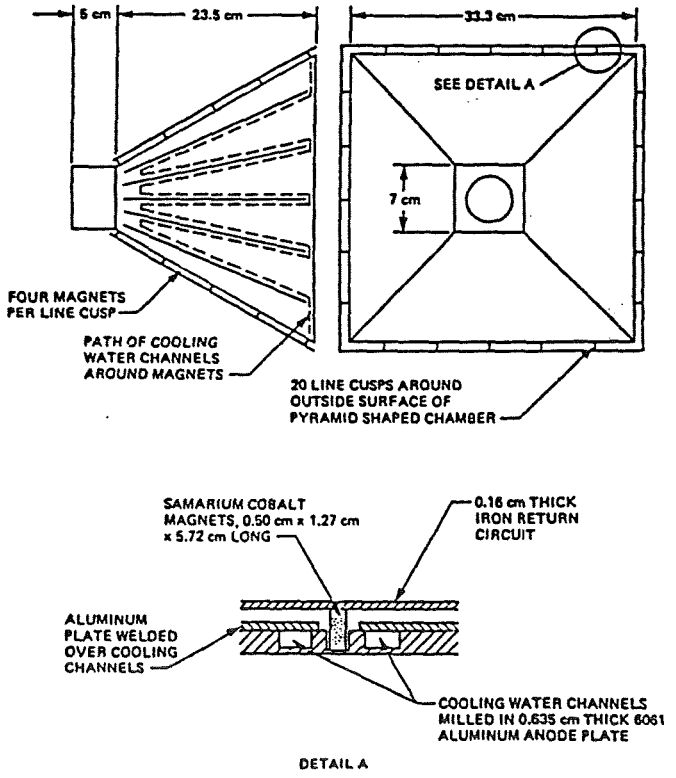

Fig. 1 Magnet retainer shell used during EPA thruster proof-of-concept tests.

A hollow cathode was designed to provide the discharge plasma electron current for the prototype EPA thruster and is shown in Fig. 2. This cathode was designed to provide maximum operating flexibility, providing emission currents of a few ampere up to over 100 ampere. This large current capability allowed a wide range of input powers to be investigated during proof-of-concept testing of the prototype EPA thruster.

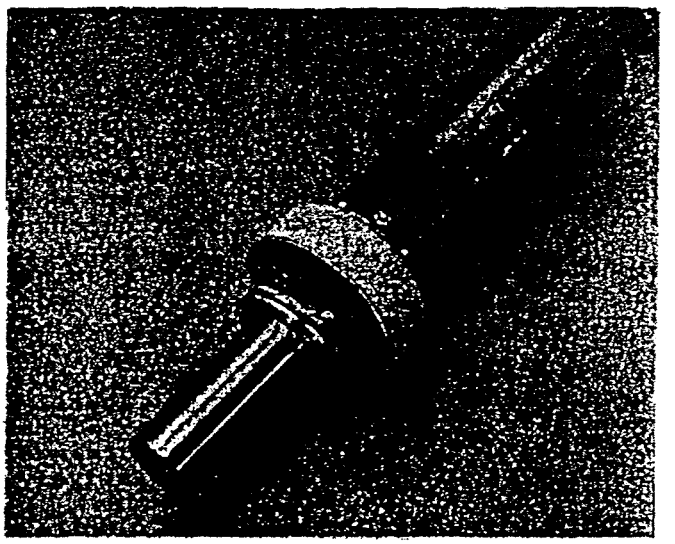

Fig. 2 Large, high current, hollow cathode used in prototype EPA thruster.

Vacuum Test Facility

Figure 3 shows the test facility used to perform the EPA thruster proof-of-concept tests. A chamber, 0.59 m in dia. and 1.83 m long, was pumped to high vacuum by a diffusion pump with a nominal pumping speed for air of 17,500 liters/sec. Backing this diffusion pump was a mechanical pumping system which included a blower and single stage roughing pump. With this vacuum tank and pumping system, background pressures were typically in the mid 10^{-5} Torr pressure range during EPA thruster operation with xenon propellant.

Power Supplies

Several power supply sets were used to operate the EPA thruster. Cathode

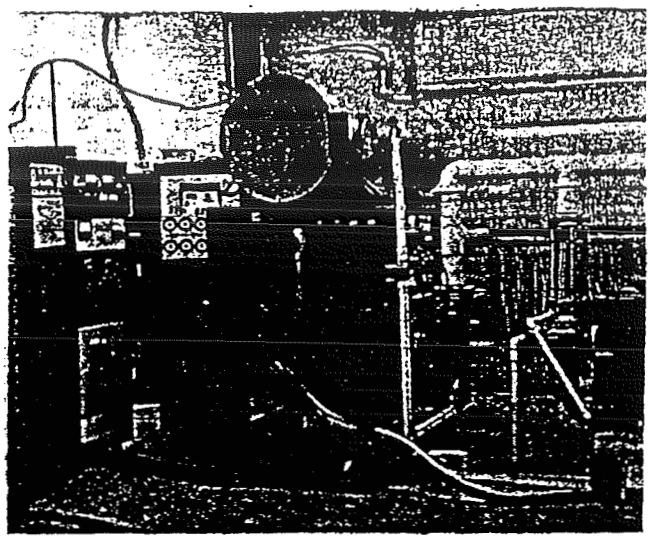

Fig. 3 Vacuum facility, power supplies and instrumentation.

heater power was provided by a ferroresonant supply which initially provided about 60 W to the heater immediately after turn-on with a gradual power increase to approximately 110 W after about 10 min. The relatively long cathode preheat time was a function of the large cathode size and mass. No attempts were made to reduce this preheat time since this was not an important consideration during this proof-of-concept test program. For cathode-to-keeper electrode breakdown and cathode start up, five series connected ferroresonant supplies provided an open circuit voltage of approximately 750 Vdc with a constant current capability of 3.5 A. As with the cathode preheat time, the cathode-to-keeper discharge starting voltage requirements were a function of the specific general purpose hollow cathode design chosen for these proof-of-concept EPA thruster tests and no attempt was made in this study to optimize this parameter.

Two sets of cathode-to-anode discharge power supplies were used during this EPA thruster test program. The first of these power supply sets comprised eleven ferroresonant power supplies each of which had a nominal output voltage of 28 Vdc and a constant current capability of 25 A. These supplies could be arranged in a variety of series and parallel combinations to simulate different spacecraft bus voltages. Figure 3 shows this power supply assembly which is incorporated into the rack at the left of this photo. The adjacent rack contains the keeper supply assembly discussed above. Next to this keeper power supply system is the second power supply set used to maintain the cathode-to-anode discharge. The principal power supply used in this rack to control the EPA thruster was a transistor regulated constant current/constant voltage unit which was always operated in the constant current mode.

Momentum Probe

To demonstrate proof-of-concept of the electrostatic acceleration process, it was necessary to quantify the thrust, specific impulse and efficiency of the prototype EPA thruster. A momentum probe was developed as a direct thrust measuring device in order to determine these parameters.

The main design features of the momentum probe are shown in Fig. 4. Plasma beam ions and neutrals from the EPA thruster impinge upon a very thin mica surface. The momentum exchanged between these particles and the mica surface exerts a small thrusting force which moves the mica probe to the left and the meter movement pointer to the right, away from its initial null position. To reestablish the meter pointer null, and therefore resolve the out of balance thrust force on the mica probe surface, a thin gold chain is unwound until the meter pointer is returned to its original null reading. The subsequent thrust force on the mica surface can then be calculated using the following trigonometric relationship:

$$T_d = (m\ f)/(2A \tan \theta)$$

In this equation, T_d is the thrust density; m is the mass increment of unwound chain; A is the area of the mica probe

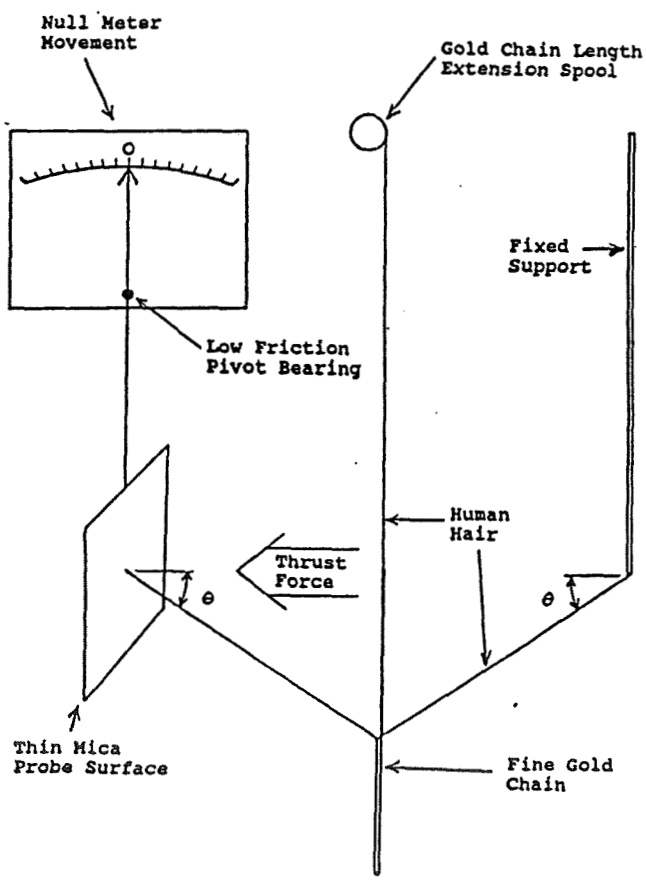

Fig. 4 Primary components of the momentum probe.

surface; θ represents the angle depicted in Fig. 4; and f is a multiplication factor that accounts for reflection of the impinging xenon particles off the mica probe surface. A value of f = 0.5 corresponds to an assumption of pure specular reflection, whereas f = 1.0 corresponds to the measured thrust density. The actual thrust density lies somewhere between these limits since the particles undergo diffuse reflection from the mica probe surface. While the probe system shown in Fig. 4 is believed to be a unique design, other workers have successfully used similar direct force measurement techniques to determine the thrust of other low thrust electric propulsion devices.[3,4]

Probe Fabrication:

Figure 5 shows the assembled momentum probe positioned in front of the EPA thruster. Construction of the probe was accomplished using a 4.1 cm x 8.2 cm thin mica plate connected directly to a microampere meter via a thin aluminum rod. A human hair was used to link the fine gold chain to the chain length extension spool as well as to the mica probe surface and the fixed support.

Fig. 5 Momentum probe mounted in front of EPA thruster.

Adjustment of the chain position was performed by rotating a flexible cable that was connected to the extension spool and a vacuum chamber feedthrough. During operation of the momentum probe, it was possible to resolve thrust differences equivalent to one link of the thin gold chain which corresponds to a mass, or thrusting force, of 2.05×10^{-3} g (2.01×10^{-5} N). The probe was mounted to a motorized carriage allowing thrust measurements to be taken at different locations along the horizontal axis of the thruster. Both the probe position in front of the thruster and the extension length of the gold chain were measured using precision potentiometers.

Cold Flow Gas Tests:

Calibration of the momentum probe was performed by measuring the cold flow specific impulse of xenon gas expanded through a conical nozzle. An illustration of the experimental set up is shown in Fig. 6. The nozzle was constructed of paper and attached to a stainless steel tube with an orifice diameter of 2.5 mm. The area ratio and half angle of the nozzle were approximately 300 and 20°, respectively.

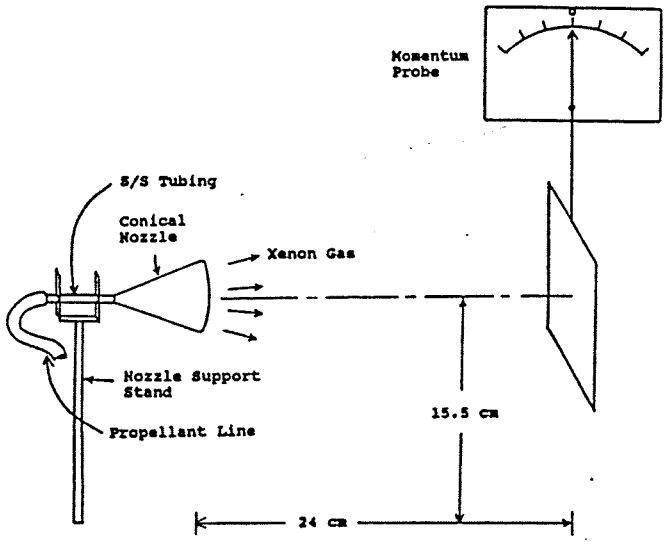

Fig. 6 Experimental setup of the cold flow specific impulse test.

The background pressure maintained in the vacuum chamber during the cold gas flow calibration experiment was 1.0×10^{-4} torr. Simple, one dimensional isentropic flow calculations indicated that a choked flow condition should exist at the throat of the nozzle at a xenon flow rate of 30 sccm. While operating the nozzle at 30 sccm, the thrust density data shown in Fig. 7 was obtained (half profiles are shown in this figure). This data corresponds to a cold flow specific impulse of 8.4 seconds (f=0.5) or 16.8 seconds (f=1.0). The actual value of the specific impulse should fall between these two values.

Expanding xenon in a well made expansion nozzle should deliver a cold flow specific impulse of approximately 25 seconds[5]. Comparing this value to the specific impulse measured with the momentum probe suggested that the probe was functioning reasonably accurately since at low mass flow rates through the nozzle, viscous effects impede the expansion of the xenon and so lower the measured thrust and specific impulse.

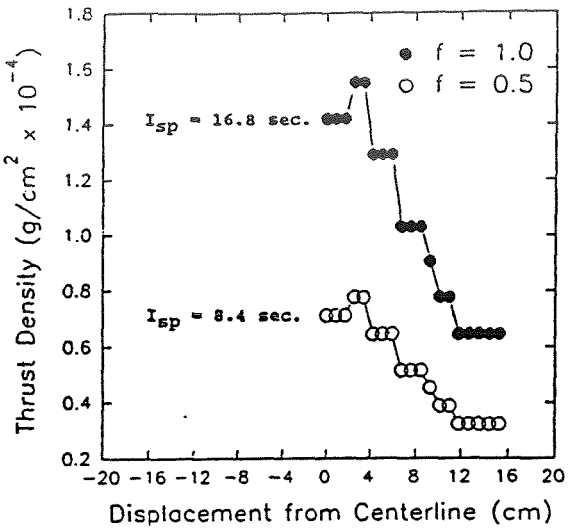

Fig. 7 Cold flow thrust density measurements.

Probe Error Analysis:

To complete the discussion describing the momentum probe, consideration must be given to the error inherent in measuring a given data point. The major factors influencing the accuracy of a thrust measurement were the measurement of the chain length, mass flow rate, exhaust area of the beam, and the angle with the horizontal subtended by the hair connecting the gold chain with the mica probe surface. Table 1 lists the uncertainty associated with each of these variables. Though the length of the gold chain could be resolved to within one link, the 3% error related to the high precision potentiometer reading corresponded to a chain length differential of about two links and was used in all error calculations. The absolute errors in thrust density, specific impulse and efficiency are shown in Table 2.

EPL Thruster Operation

The first set of runs with the EPA thruster were used to verify operation of the momentum probe and to investigate the effects of different parameters on thruster operation. Upon analyzing the data to determine thrust, specific impulse, and efficiency, subsequent modifications were made to the thruster configuration in order to further study thruster performance. During these tests, the thruster was started 55 times, accumulating a total run time of 9 hours and 40 minutes. Results of several of these tests are summarized below.

Preliminary Tests:

Initial tests of the EPA thruster included a total of 20 data runs in which several thruster operating parameters were varied during operation of the momentum probe. The momentum probe was extremely stable during transit across the thruster exit plane and the typical time required to obtain a probe thrust density measurement was approximately 30 seconds. Specific thruster operating conditions corresponding to these separate runs are presented in Table 3. Runs #1 - #5 showed thrust density profiles within the EPA thruster plasma exhaust. Due to a mechanical problem in the probe carriage, data runs #6 through #12 shown in Table 3 were taken at a fixed position in front of the thruster.

Table 1
Uncertainty in Momentum Probe Parameters.

Variable	Uncertainty
Chain length	± 1 link
Potentiometer reading	± 3 %
Hair angle, θ	± 1°
Beam radius	± 2 cm
Mass flow rate	± 1 sccm

Table 2
Percent Error in Performance Parameters.

Parameter	% error lower bound	% error upper bound
Thrust density	-26 %	+29 %
Specific impulse	-36 %	+50 %
Efficiency	-61 %	+136 %

Table 3
Preliminary EPA Thruster Performance Tests.

$\dot{m}_c$ sccm	$\dot{m}_m$ sccm	V_D V	I_D A	f = 0.5 T g(10^{-4})	I_{sp} sec	Eff %	
12	80	0	0	0.20	17.6	-	*
12	80	0	0	0.30	25.8	0.35	§
12	80	0	0	0.44	37.8	0.42	▼
6	40	0	0	0.24	39.0	0.20	▼
6	40	40	10	0.48	76.6	0.32	▲
6	40	43.5	15	0.54	87.6	0.28	▲
6	40	40	10	0.44	71.4	0.19	▲
6	40	47	20	0.64	104	0.30	▲
6	40	51	25	0.80	130	0.35	▲
6	30	45.5	15	0.48	96.4	0.27	▲
6	50	40	15	0.58	79.0	0.30	▲
3	50	41	15	0.62	87.8	0.34	▲
6	50	47	25	0.84	111	0.56	▲
6	50	46.5	30	1.00	133	0.44	▲

Comments: * cold gas flow
§ heater on
▼ heater/keeper on
▲ discharge on

The analysis used to produce the specific impulse and efficiency numbers listed in Table 3 was deliberately very conservative. For example, the thruster mass flow rate was assumed to include the mass flow rate of background gas from the vacuum tank which was assumed to be re-ingested by the thruster. This calculated background mass flow rate is a function of facility pressure and was assumed to be composed entirely of xenon. For these preliminary data, EPA thruster performance calculations were performed assuming purely specular reflection off the probe wherein the measured thrust density values were halved, that is f was assumed to be 0.5. Given these assumptions, Table 3 shows that maximum specific impulse values of 100 - 130 sec. were achieved. Note that the accuracy of these larger specific impulse values obtained during runs #6 - #12 was questionable since only one thrust density point was taken per run and the exhaust plume area was only approximated.

Propellant Manifold Redesign:

After the initial set of data runs, it was realized that one contributor to the low values of specific impulse measured in Table 3 was the thruster propellant injection configuration and the small plasma production volume caused by the far downstream cathode axial position. To overcome these problems, the cathode was relocated far back in the rear of the thruster and the downstream propellant injection manifolds were replaced by a single propellant injection manifold that surrounded the rear of the cathode. This revised EPA thruster configuration is pictured in Fig. 8.

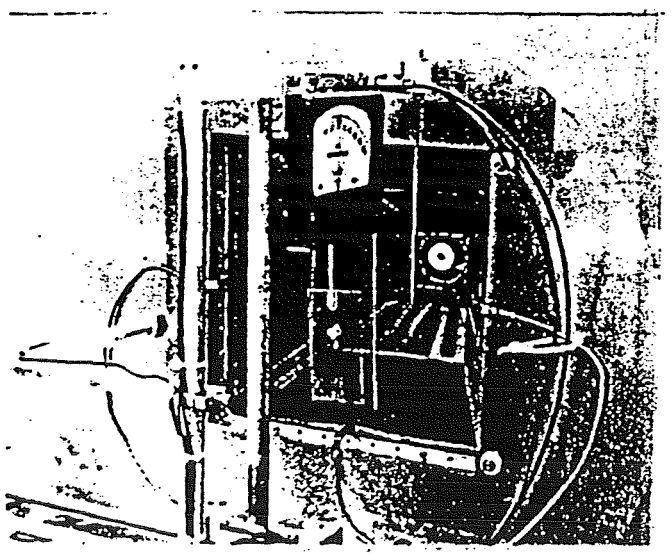

Fig. 8 EPA thruster with relocated cathode and propellant manifold.

Figure 9 documents the discharge current and voltage characteristics of the modified EPA thruster as a function of the propellant flow rate through the cathode and rear manifold. Comparing the results of Fig. 9 with those from Table 3 shows similar discharge current and voltage characteristics are attained with this reworked EPA thruster configuration but that the required propellant flow rates have been reduced by a factor of four. The results of Fig. 9 also show that for a fixed manifold flow rate and discharge current, the discharge voltage was reduced substantially as the cathode flow rate was increased (squares, upside down triangles and diamonds).

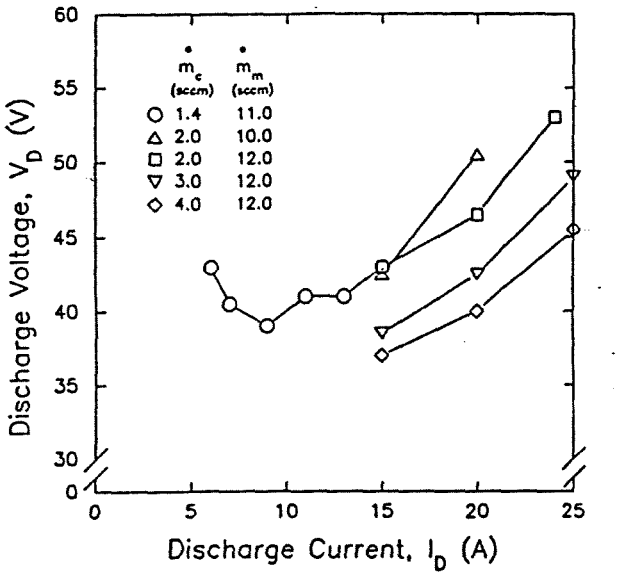

Fig. 9 EPA thruster discharge V-I characteristics after reducing the thruster propellant flow rate requirement by a factor of four.

In addition to modifying the propellant injection manifold, the thruster ground screen was also modified slightly in Fig. 8 compared to the preliminary thruster configuration shown in Fig. 5. Figure 10 shows thrust density profiles corresponding to various operating conditions of the thruster configuration shown in Fig. 8. Data at a discharge voltage of 41 V were taken within several minutes of each other with the thruster at the same operating conditions. These runs show that the reproducibility of the momentum probe measurement system was very good. Also in Fig. 10, the effect of turning off the cathode heater was seen to increase the discharge voltage and discharge power. This voltage and power increase reflects the plasma compensating for the lack of heater power by increasing the energy of the backstreaming ions to the cathode to increase cathode self-heating by ion bombardment.

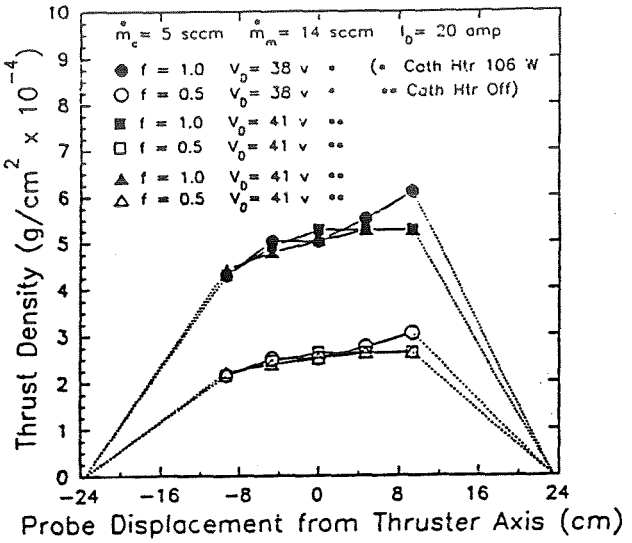

Fig. 10 Thrust density profiles after propellant manifold and ground screen modifications.

Figure 10 shows that the thrust density profiles are skewed. This behavior was directly related to the plasma distribution within the thruster which was non-uniform. Because of this plasma non-uniformity, a data analysis procedure was applied to the thrust density profiles shown in Fig. 10, and later results, wherein a straight line drop-off was assumed between the last probe data point and the beam edge (dotted lines in Fig. 10). The beam edge was determined by a separate ion flux probe in the same plane as the momentum probe but positioned far enough off the thruster axis to detect the accelerated plasma exhaust boundary. The thrust density data was analyzed by integrating under the profiles shown in Fig. 10 to obtain total thrust and then using this thrust value to calculate specific impulse and efficiency. Table 4 shows the results of these calculations for f = 0.5 and f = 1.0 (corresponding to the actual measured thrust density). Comparing these results with the cold flow specific impulse measurements of Fig. 7, shows more than an order of magnitude increase in specific impulse.

Magnet Removal:

Visual examination of the EPA thruster showed a severe non-uniform plasma discharge which was evidenced by the skewed thrust density profiles shown in Fig. 10. In particular, most of the discharge was seen to concentrate in opposite corners of the thruster. Figure 11 shows a picture of the thruster operating with this severely non-uniform plasma. Superimposed on this tendency to concentrate plasma production in opposite corners, was an additional effect wherein every second magnet line cusp showed no visible evidence of plasma luminosity.

Table 4
EPA thruster performance tests with partial optimization of propellant injection system and modified ground screen

	f = 0.5			f = 1.0		
V_D V	Thrust g(10^{-4})	I_{sp} sec	Eff %	Thrust g(10^{-4})	I_{sp} sec	Eff %
38	0.33	117	0.22	0.66	234	0.86
41	0.31	108	0.19	0.61	215	0.77

Comments: $\dot{m}_c$ = 5 sccm
$\dot{m}_m$ = 14 sccm
I_D = 20 A

Fig. 11 Thruster operation showing plasma concentration in large corner cusps.

Inspection of the magnetic field distribution in the corner of the EPA thruster suggested that the second row of magnets in from each corner may have been short circuiting the magnet cusp at the corners, effectively eliminating these cusps from the discharge. To overcome this problem, all corner magnets were removed from the magnet retainer shell. Figure 12 shows a photograph of thruster operation following this change and clearly shows much less concentration of the plasma at the corners. However, this figure still shows the alternating magnet cusp luminosity and subsequent plasma non-uniformity which appeared to be a permanent feature of the pyramid shaped magnet retainer design.

Table 5 shows the thruster performance parameters calculated after the magnets were removed. Of most interest is the large relative efficiency increase caused by small flow rate changes. In particular, stable thruster operation was achieved at a discharge voltage of 38 V. These data

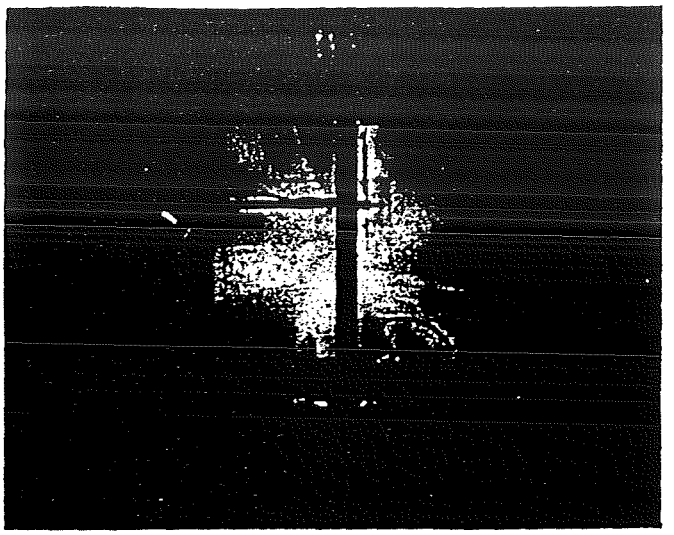

Fig. 12 Thruster operation after magnet removal showing absence of large plasma filled corner cusps but still showing alternating magnet cusps with and with out plasma present.

Table 5
Thruster performance parameters after magnet removal

f = 0.5			f = 1.0			
Thrust $g(10^{-4})$	I_{sp} sec	Eff %	Thrust $g(10^{-4})$	I_{sp} sec	Eff %	
0.25	89	0.14	0.49	178	0.55	*
0.28	94	0.22	0.55	189	0.88	§

Comments: $\dot{m}_c$ = 2 sccm
I_D = 15 A
* $\dot{m}_m$ = 17 sccm and V_D = 51 V
§ $\dot{m}_m$ = 21 sccm and V_D = 38 V

suggested that discharge voltages of order 28 V could be expected with further thruster design optimization.

Comparison with the results of Table 4, shows that specific impulse did not decrease significantly following removal of the corner magnets. Since one third of the magnets were removed from the engine in making this change, this behavior suggests that the discharge chamber magnetic field geometry was far from an optimum configuration. Poor plasma electron magnetic field containment was the principle reason for very low thruster efficiency values during this proof-of-concept program.

Discharge Chamber Masking:

After testing the thruster with the corner magnet cusps removed, a mica mask of 20 cm dia. was placed over the thruster exit plane. The purpose of this test was to pressurize the discharge chamber by preventing direct escape of a portion of the neutral propellant. A photograph of the masked down thruster during operation is shown in Fig. 13.

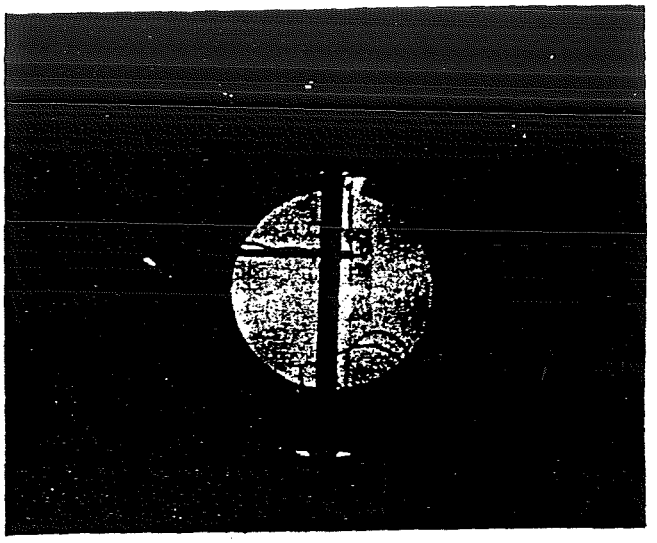

Fig. 13 Thruster operation with circular mica mask over the discharge chamber exit plane.

Figure 14 plots the measured thrust density characteristics of the masked down EPA thruster. The thruster performance parameters calculated for these profiles are presented in Table 6. It should be noted that only one data point was obtained at a discharge current of 30 A and then the momentum probe hair broke allowing the gold chain to be lost to the inside of the vacuum system diffusion pump. This single data point was analyzed by assuming a thrust density profile identical in form to that obtained with a 25 A discharge current.

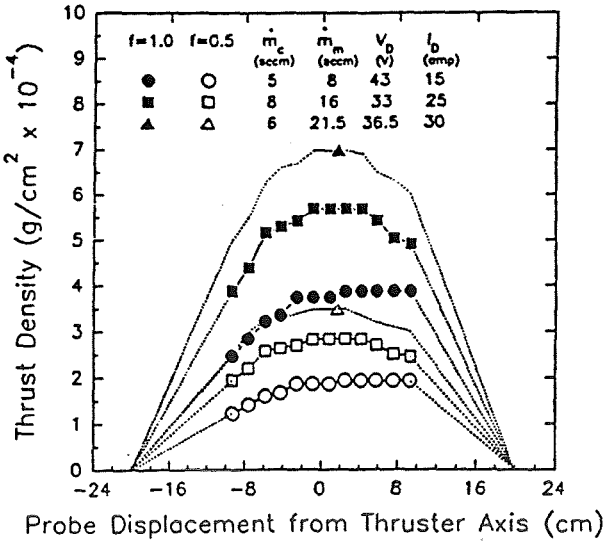

Fig. 14 Thrust density profiles with masked down EPA thruster.

Table 6
Thruster performance parameters after fitting mica mask over the discharge chamber exit plane

$\dot{m}_c$ sccm	$\dot{m}_m$ sccm	V_D V	I_D A	f = 0.5 Thrust g(10^{-4})	f = 0.5 I_{sp} sec	f = 0.5 Eff %	f = 1.0 Thrust g(10^{-4})	f = 1.0 I_{sp} sec	f = 1.0 Eff %
5	8	43	15	0.13	74	0.06	0.25	148	0.24
8	16	33	25	0.18	59	0.05	0.35	117	0.21
6	21.5	36.5	30	0.27	83	0.09	0.55	166	0.36

In general, thruster performance with the discharge chamber mask was worse than without it. This occurred since the mica mask created a very large surface for discharge plasma recombination with correspondingly large reductions in plasma production efficiency. Nevertheless, data shown with a 15 A discharge current is significant because stable thruster operation was achieved at relatively low flow rates. The cathode heater was turned off while operating at a 15 A discharge current. After several minutes, thruster operation stabilized at a discharge voltage of 51 V. These conditions represented a discharge power increase of 120 W which was similar to the normal cathode heater power requirement of 106 W. This large cathode power requirement was a further cause for very low thruster efficiency values during this program.

Summary

A systematic experimental program was undertaken to investigate thrusting effects caused from electrostatic plasma acceleration from a moderately dense plasma discharge. Preliminary results obtained with prototype hardware showed accelerated plasma specific impulse levels at least an order of magnitude larger than could be achieved by cold gas flow expansion. While thruster efficiency levels were very low this appeared to be a result of the inherent operating power requirements and geometrical deficiencies in the prototype hardware used for this investigation. Reliable EPA thruster operation was achieved using one power supply.

Acknowledgement

This work was supported by the Center for Advanced Space Propulsion (CASP) under subcontract CAR/EPL 89-01, and by in-kind support from the Electric Propulsion Laboratory, Inc.

References

1. Kerslake, W. R. and Ignaczak, L. R., "SERT II 1980 Extended Flight Test Thruster Experiments," AIAA Paper No. 81-0665, April 1981.

2. Aston, G. and Deininger, W. D., "Test Bed Ion Engine Development," NASA CR-174623, March 1984.

3. Snyder, A. and Banks, B.A., "Thrust measurements of a hollow cathode discharge", NASA TN D-6705, March 1972.

4. Nakanishi, S., Private communications, Mar.-April 1990.

5. Holcomb, L. B., "Satellite Auxiliary Propulsion Selection Techniques," JPL Tech. Rep. No. 32-1505, Nov. 1970.